Physiol Genomics
5: 161–170, 2001.

Monitoring expression of genes involved in drug metabolism and toxicology using DNA microarrays

DAVID GERHOLD,[1] MEIQING LU,[1] JIAN XU,[1] CHRISTOPHER AUSTIN,[1]
C. THOMAS CASKEY,[1] AND THOMAS RUSHMORE[2]
[1]*Pharmacology Department and* [2]*Drug Metabolism Department,*
Merck Research Laboratories, West Point, Pennsylvania 19486

Received 12 September 2000; accepted in final form 15 February 2001

Gerhold, David, Meiqing Lu, Jian Xu, Christopher Austin, C. Thomas Caskey, and Thomas Rushmore. Monitoring expression of genes involved in drug metabolism and toxicology using DNA microarrays. *Physiol Genomics* 5: 161–170, 2001.—Oligonucleotide DNA microarrays were investigated for utility in measuring global expression profiles of drug metabolism genes. This study was performed to investigate the feasibility of using microarray technology to minimize the long, expensive process of testing drug candidates for safety in animals. In an evaluation of hybridization specificity, microarray technology from Affymetrix distinguished genes up to a threshold of ~90% DNA identity. Oligonucleotides representing human cytochrome *P*-450 gene *CYP3A5* showed heterologous hybridization to *CYP3A4* and *CYP3A7* RNAs. These genes could be clearly distinguished by selecting a subset of oligonucleotides that hybridized selectively to *CYP3A5*. Further validation of the technology was performed by measuring gene expression profiles in livers of rats treated with vehicle, 3-methylcholanthrene (3MC), phenobarbital, dexamethasone, or clofibrate and by confirming data for six genes using quantitative RT-PCR. Responses of drug metabolism genes, including *CYP*s, epoxide hydrolases (*EH*s), UDP-glucuronosyl transferases (*UGT*s), glutathione sulfotransferases (*GST*s), sulfotransferases (*ST*s), drug transporter genes, and peroxisomal genes, to these well-studied compounds agreed well with, and extended, published observations. Additional gene regulatory responses were noted that characterize metabolic effects or stress responses to these compounds. Thus microarray technology can provide a facile overview of gene expression responses relevant to drug metabolism and toxicology.

DNA microarray; drug metabolism; gene regulation; cytochrome *P*-450

LIVER IS A PRIMARY SITE for drug and hormone metabolism, for coordination of energy metabolism and for a variety of exocrine and endocrine functions. Within the liver, cytochrome *P*-450 (*CYP*) genes are dynamically regulated in response to diet, xenobiotics, and hormonal balance. Because *P*-450s are regulated by many such signals at the transcriptional level, steady-state mRNA levels of the *P*-450s and other drug-metabolizing enzymes in liver reflect the overall state of the organism. The dynamic regulation of liver genes led us to design both a "Merck Drug Safety Chip" and a database to apply DNA microarray technology to drug metabolism and to interrelated toxicology and energy metabolism issues.

Metabolism of xenobiotics and steroid hormones is carried out in three "phases" (12). Drug-metabolizing enzymes modify substrates directly via oxidation, hydroxylation, and dealkylation (phase I enzymes), by conjugating drugs to sulfate, glutathione, or carbohydrates to facilitate clearance (phase II enzymes), and by directional transport of these conjugates from liver into the bile or urine (phase III enzymes). We focused initially on the cytochromes *P*-450, including *CYP3A*, *CYP2D*, *CYP2C*, and *CYP4A* family members, that collectively metabolize ~90% of commercial drugs (7). Since genetic variations, polymorphisms, are common in several of the important *CYP* genes in human populations, it is important to be able to monitor regulation of these enzymes in clinical subjects. The presence of inactive alleles can lead to persistence of drugs in susceptible subjects leading to potential adverse reactions. Inactive alleles in *CYP2C9*, for example, lead to persistence and life-threatening toxicity of warfarin levels in serum. (13) Thus it is important to understand which enzymes metabolize a drug candidate.

A drug that is metabolized by a given cytochrome *P*-450 frequently induces expression of that *P*-450 at the transcriptional level (34). Induction of particular cytochromes *P*-450 in the liver can herald either harmful or benign clinical events. Although existing enzymatic assays and mass spectrometric analyses are necessary to determine which gene subfamily is actually metabolizing a given compound, these assays often fail to distinguish gene subfamily members. DNA microarray assays are thus complementary to enzymatic assays, as they help provide a prediction of which genes are metabolizing the drug and a facile overview of the liver's responses to the drug. DNA microarray assays could also be used to compare transcriptional changes caused by drugs to identify therapeutic mechanisms and potential side effects (20). If a compound causes an adverse effect, then transcriptional changes in the liver may provide clues to the mechanism of the toxic insult.

Article published online before print. See web site for date of publication (http://physiolgenomics.physiology.org).

Address for reprint requests and other correspondence: D. Gerhold, Merck, WP26A-3000, Broad St. and Sumneytown Pk., West Point, PA 19486 (E-mail: david_gerhold@merck.com).

Such insults may be oxidative, tumor initiating or promoting, or inflammatory, for example.

DNA microarray technology typically encompasses arraying of DNA on a glass surface, hybridization and detection methods, and software and databases that facilitate data analyses. DNA microarrays representing thousands of genes can be hybridized to fluorescence-labeled samples representing mRNA populations from control and experimental tissues (11). Expression of each surveyed gene is detected and quantitated as fluorescence from the hybridizing nucleic acid. It should be noted that such data represent steady-state mRNA abundance, reflecting both changes in transcription rate and rate of message destruction. Differentially expressed genes can be identified by informatic comparison of control and experimental hybridization data. Such data can be maintained in relational databases to allow queries to be performed on any or all data simultaneously.

Effective methods have been developed for spatially addressed synthesis of short oligonucleotides, or mechanical arraying of cDNA inserts, on derivatized glass surfaces (10, 27). Synthetic oligonucleotides allow rational avoidance of DNA sequences that are shared by several genes or repeated in the genome. The 25-mer oligonucleotide GeneChip microarray format of Fodor et al. (10) was used in the studies described, due to its potential for discriminating between the closely related gene sequences prevalent in drug metabolism gene families.

Interpretation of complex transcriptional responses to xenobiotics and subsequent prediction of physiological effects is currently problematic. Drawing links between gene expression profiles and physiological effects demands formation of a database using compounds with well-characterized effects from a variety of mechanistic classes. To demonstrate the feasibility and validity of this approach, we examined the responses of drug metabolism genes in the rat liver to four well-studied compounds [3-methylcholanthrene (3MC), dexamethasone, phenobarbital, and clofibrate] using DNA microarrays.

MATERIALS AND METHODS

DNA microarray design and synthesis. For the Merck Drug Safety Chip, 1,443 genes were selected in aggregate from rat, human, and mouse for their roles in drug metabolism, toxicology, and energy metabolism in liver tissue. Among the 300 rat genes included in the Merck Drug Safety Chip design are 130 genes classified as drug-metabolizing genes, including 51 *CYP* genes and 79 phase II and phase III drug-metabolizing genes and gene splice forms. In vehicle-treated rat liver samples, expression is detected for approximately one-third of the 300 rat genes represented on the Merck Drug Safety Chip. Each gene on the Merck Drug Safety Chip is represented by 20 pairs of 25-mer oligodeoxyribonucleotide "probes." Each probe pair consists of a perfect match (PM) oligonucleotide that precisely matches the cognate gene sequence and a mismatch (MM) oligonucleotide that differs only in a single nucleotide mismatch in the center position. Selection of probes and manufacture of the GeneChips was performed by Affymetrix (Santa Clara, CA). (For the sequences of twelve PM 25-mer probes that yielded gene-specific hybridization for human CYP3A5, please refer to the Supplementary Material[1] for this article, published online at the *Physiological Genomics* web site.)

Rat treatment protocols. Sprague-Dawley rats were purchased from Charles River Laboratories, Wilmington, MA. Rats were watered and fed chow ad libitum. Animal treatments were reviewed and approved by the Institutional Animal Care and Use Committee. Rats were dosed orally once per day for 3 days with 0.1% methylcellulose vehicle or 30 $mg \cdot kg^{-1} \cdot day^{-1}$ of 3MC, dexamethasone, phenobarbital, or clofibrate. On *day 4*, rats were killed, and livers were harvested and frozen immediately on dry ice. mRNA was isolated from individual livers of at least two rats per treatment.

RNA preparation. Tissues were homogenized in Trizol (Life Technologies, Gaithersburg, MD) using a Polytron (Omni International, Warrenton, VT), and total RNA was isolated from each sample according to the manufacturer's instructions. Total RNA was reprecipitated using RNAmate (Biochain, San Leandro, CA); mRNA was isolated using oligo-dT-decorated latex beads (Qiagen, Hilden, Germany) according to the manufacturer's instructions.

Hybridization and staining. Hybridization samples were prepared according to Affymetrix instructions as described (18). Briefly, a primer encoding the T7 RNA polymerase promoter linked to oligo-dT_{17} was used to prime double-stranded cDNA synthesis from each mRNA sample using Superscript II RNase H^- reverse transcriptase (Life Technologies, Rockville, MD). Each double-stranded cDNA sample was purified by adsorption to silica (Qiaquick kit, Qiagen) according to manufacturer's instructions, then in vitro transcribed using T7 RNA polymerase (MEGAscript T7 kit; Ambion, Austin, TX), incorporating biotin-UTP and biotin-CTP (Enzo Biochemicals, New York, NY) into the resulting copy RNA (cRNA). These cRNA transcripts were purified using RNEasy (Qiagen) and quantitated by measuring absorption at 260 nm/280 nm. Five-microgram mRNA samples typically yielded between 30 and 150 μg purified cRNA. cRNA samples were fragmented at 95°C for 35 min in 10 mM $MgCl_2$ to a mean size of ~50–100 nucleotides, added to hybridization buffer, and hybridized to the Merck Drug Safety Chip for 16 h at 45°C. GeneChips were washed, stained with streptavidin-R-phycoerythrin, and scanned with a dedicated instrument to capture a fluorescence image (Molecular Dynamics).

Hybridization spikes. Biotinylated RNA samples were prepared from individual *CYP* genes to spike into hybridization samples at known concentrations, as follows. *CYP3A* gene expressed sequence tag (EST) clones that contained the entire 1,000 nt 3′ region represented on the GeneChips were selected. GenBank accession numbers for the *CYP3A* clones were as follows: *CYP3A4*, no. T60335; *CYP3A5*, no. AA740526; and *CYP3A7*, no. AA455159. The *CYP* gene and the cDNA clones in vector pCDNA3.1 were obtained from the following: Frank Gonzalez, National Institutes of Health, supplied *CYP2A6*, GenBank no. M33318; Joyce Goldstein National Institute of Environmental Health Sciences, supplied *CYP2C19*, GenBank no. M61854; and Tom Rushmore supplied *CYP2D6*, which is unpublished. The inserts from *CYP3A4* (in pBluescript SK−; Stratagene, La Jolla, CA), *CYP3A5*, and *CYP3A7* (EST clones in pT7T3D-Pac; Ref. 30) or full-length clones in pCDNA3.1 (Invitrogen, Carlsbad, CA) were amplified by PCR using primers that match DNA sequences flanking the cDNA insertion sequences in each

[1] Supplementary Material to this article is available online at **http://physiolgenomics.physiology.org/cgi/content/full/5/4/161/DC1**.

vector. PCR primers were the "T7" primer (5′ TAATACGACTCACTATAGGG) and a "T3-pCDNA3.1" primer (for pCDNA3.1: 5′ AGATGCAATTAACCCTCACTAAAGGGAGAGAAGGCACAGTCGAGGCTGA) or a "T3" primer (for EST clones: 5′ ATTAACCCTCACTAAAGGGA) that encodes a T3 RNA polymerase promoter sequence. PCR products were purified by adsorption to silica (Qiaquick kit, Qiagen) according to the manufacturer's instructions. Each PCR product was then transcribed in vitro to generate the antisense strand of each gene using T3 RNA polymerase for pCDNA3.1 and pT7T3D-Pac or using T7 RNA polymerase for pBluescript SK−, incorporating biotin-UTP and biotin-CTP into the resulting cRNA. These cRNA transcripts were purified using RNEasy (Qiagen), quantitated by measuring absorption at 260 nm/280 nm, and spiked into hybridizations at known concentrations.

GeneChip data analysis. Data from each microarray were normalized to data from a single vehicle microarray using global scaling based on the overall hybridization intensities. Normalization, assessments of replicates, and calculations of gene expression levels as average difference values were performed using GeneChip v. 3.1 software. Each treatment was represented by two replicate samples, using three pooled rat livers per sample and two microarrays.

Quantitative RT-PCR. TaqMan quantitative reverse transcriptase PCR (Q-RT-PCR) was used to quantitate mRNA levels for selected genes as described in detail by Wang and Brown (33). Two primers and one probe were designed for each gene using Perkin-Elmer PrimerExpress v. 1.0 software.

Primer and probe sequences are listed for forward primers "_F", reverse primers "_R", and probes "_M" which were labeled with 6-carboxyfluorescein (FAM) on the 5′ nucleotide and 6-carboxy-*N,N,N′,N′*-tetramethylrhodamine (TAMRA) on the 3′ nucleotide.

*APOA1*_F GTTTGGGCTCTACAGCGATCAG
*APOA1*_R TGGTTCTTGATCTCGGTCAGG
*APOA1*_M TGCGCGAGAACCTGGCCCA

*BE*_F CCTCTGAAGGAATGGCAAAGC
*BE*_R CGCAGAAGGCTGAATCACAG
*BE*_M CAGGGCCCCACGGCAGCA

*CYP1A1*_F GGAGGTGCTCTTGCCATCTG
*CYP1A1*_R CACCCCCACATGTAGTGTCATAA
*CYP1A1*_M TGAGGCTCAACTGTCTTCCAACATGGG

*CYP3A18*_F TGGCATGAGGTTTGCTCTCA
*CYP3A18*_R TCACAAGGCTGGATATTGAAGTTC
*CYP3A18*_M CAGCATGAAACTTGCTGTCATAGGAGTCCTG

*GSTM1*_F AGACAGAGGAGGAGCGGATTC
*GSTM1*_R GCTGCATGCGGTTGTCC
*GSTM1*_M TGCCGACATTGTGGAGAACCAGGTC

Assays were run on the Perkin-Elmer ABI 7700 instrument under default conditions. Abundance of each gene was determined relative to a standard transcript, 18S rRNA. cDNA was prepared from two pools of three livers per treatment group, and each cDNA was assayed in duplicate PCR reactions.

Quantitative RT-PCR data analysis. Average C_t values from duplicate PCR reactions were normalized to average C_t values for 18S rRNA from the same cDNA preparations. The ratio of expression of each gene in drug-treated vs. vehicle-treated samples was calculated as $2^{-(\text{mean}\Delta\Delta C_t)}$ of that treatment as recommended by Perkin-Elmer where C_t is the threshold cycle, and $\Delta\Delta C_t$ is the difference C_t(test gene) − C_t(18S rRNA) for treated sample minus vehicle sample. Using the ANOVA method, 95% confidence intervals were determined for each ratio as

$$2\ \exp\left[-(\text{mean}\Delta\Delta C_t) \pm t_{0.025,N-m}\sqrt{\frac{1}{n_i}+\frac{1}{n_j}}\right]$$

where t is the inverse of t distribution for the specified degree of freedom $N - m$, N is the total pooled sample size within a gene, m is the number of treatments including control within a gene, s is the pooled standard deviation, and n_i and n_j are the independent sample sizes in control and treated groups, respectively.

RESULTS AND DISCUSSION

Data confidence. Each gene is represented on the Merck Drug Safety Chip by 10–60 pairs of 25-mer oligodeoxynucleotides, or "probes." One 25-mer of each pair is a "perfect match" (PM) to the gene sequence, and the other "mismatch" (MM) differs from the first only at the central (13th) nucleotide. The difference in hybridization, PM minus MM, is an indication of specific hybridization. In a hybridization experiment, PM-and-MM pairs are discarded if the difference PM − MM < 20 or the quotient PM/MM < 1.2. The expression level of a gene is represented empirically as the average of the PM minus MM values for all 25-mer pairs that lie within 3 standard deviations of the mean of the probe set for that gene (8).

Despite this redundancy, some experimental variation is observed in gene expression levels even in replicate hybridizations of the same sample. Such variation can lead to identification of "false positives." We use the following empirical cutoff values to screen out false positives: the absolute expression levels (average difference values) between two hybridizations differ by ≥20 units and by a ratio of ≥2-fold. We derived these criteria from previous experiments in which pairs of hybridization samples were derived from a common mRNA sample and hybridized to replicate microarrays. In these experiments, the false-positive rate ranged from 0.4–1.8% of genes detected using these criteria (unpublished observations). If false-positive events in different hybridization samples arise independently, then two replicates of each sample would yield a false-positive rate of 0.16 to 4 per 10,000. Thus replication of samples is an efficient method by which to identify false positives that arise independently. Experiments in which multiple samples were analyzed from each single liver indicate that interindividual biological variation exceeds experimental variation in this biological system. Hence, three livers were pooled for analysis on each microarray. Such data also suggest that a subset of genes detected are hypervariable between individuals, although very large data sets will be required to define levels of interindividual variation and assign levels of variability to particular genes.

Gene specificity. We tested the ability of the Affymetrix technology to discriminate between closely related genes using the large *CYP* gene family. DNA homology relationships between the 3′ 1,000 bp of

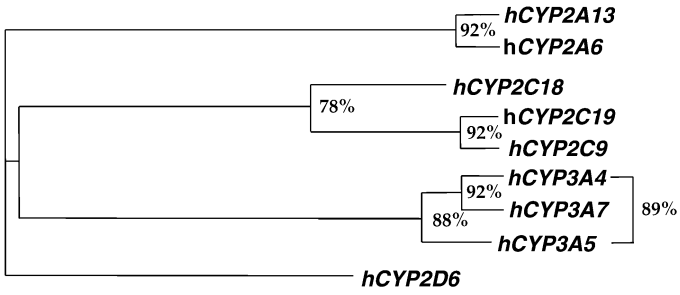

Fig. 1. DNA sequence similarities among human *CYP* (cytochrome *P*-450) genes. This dendrogram relates DNA homologies between genes from four *CYP* subfamilies: *CYP2A*, *CYP2C*, *CYP2D*, and *CYP3A*. Each family is represented on the GeneChips used in these studies. The pair-wise percent DNA sequence identities between the 3′ 1 kb of each gene within subfamilies are indicated. The ClustalW algorithm was used with gap opening penalty = 15, gap extension penalty = 6.66, and gap separation penalty range = 8.

some human cytochromes *P*-450 examined in this study are depicted in Fig. 1. Probe sequences representing each gene were selected for predicted hybridization efficiency and filtered to exclude probe sequences that are complementary to >23 of 25 bases in other gene sequences represented on the same microarray. Probe specificity was evaluated using a microarray designated "Merck-1" that represents each of 32 human *CYP* genes by 60 probe pairs from the 3′-terminal 1,000 bases of each gene sequence. Biotin-labeled RNAs were prepared by in vitro transcription of cDNA clones for human genes: *CYP2A6*, *CYP2C19*, *CYP2D6*, *CYP3A4*, *CYP3A5*, and *CYP3A7*. These biotin-RNAs were combined in sets of four to include one *CYP3A* gene (*CYP3A4, CYP3A5,* or *CYP3A7*) per set and hybridized to microarray "Merck-1." Each transcript was used at 30 pM in a 200-μl hybridization sample. Under these conditions, 30 pM corresponds to roughly 1 part in 5,000 in an mRNA population, or about 60 transcripts per mammalian cell.

Probes representing the *CYP2A6*, *CYP2C19*, *CYP2D6*, *CYP3A4*, and *CYP3A7* genes hybridized faithfully and selectively to their cognate genes. These genes did not hybridize significantly to other human *CYP* genes present on the array. The *CYP3A5* probe set, however, showed significant heterologous hybridization to *CYP3A4* and *CYP3A7* (Fig. 2). On average, the *CYP3A5* probes showed a 2.5-fold reduced hybridization to *CYP3A7* and a 10-fold reduced hybridization to *CYP3A4*. Probes representing the *CYP3A4* gene hybridized approximately fivefold less robustly to the *CYP3A4* RNA compared with probes for the other five genes examined with their cognate RNAs (Fig. 2). This may be a consequence of the stringent selection of gene-specific probes for this gene.

The data were examined in detail, to determine whether individual *CYP3A5* probe pairs distinguish this gene from *CYP3A4* and *CYP3A7*. Figure 2*B* compares hybridization (PM-MM) of probes representing *CYP3A5* on the microarray, to probes for *CYP3A4*, *CYP3A5,* and *CYP3A7*. Probe pairs 20, 21, and 42–44 show strong heterologous hybridization to two or all three human *CYP3A* genes, whereas probe pairs 18, 33–37, 45, 50, and 54–60 hybridize poorly to each of the three human *CYP3A* genes. Nevertheless, probe pairs 3–6, 8, 15, 16, 25, 48, 49, 52, and 53 show robust hybridization to *CYP3A5*, at a gene-selectivity ratio of 10-fold or greater. These latter twelve probe pairs can be used to distinguish *CYP3A5* from the other human *CYP3A* genes. Sequences for these twelve probe pairs are listed at the *Physiological Genomics* web site (see the URL in footnote 1, in the MATERIALS AND METHODS).

The cross-hybridization among CYP3A genes, but not other gene subfamilies with similar homologies (compare Fig. 1 and Fig. 2), was unexpected. The relatively poor gene specificity of probes representing *CYP3A5* may have been a consequence of the short 3′-untranslated region (3′-UT) used to design probes

A

Chip Probes:	Genbank Accession:	Spiked genes: *CYP2A6, CYP2C19, CYP2D6, CYP3A4*	*CYP2A6, CYP2C19, CYP2D6, CYP3A5*	*CYP2A6, CYP2C19, CYP2D6, CYP3A7*
CYP2A6	X13897	**2938**	**2892**	**3153**
CYP2A13	U22028	1	0	0
CYP2C8	Y00498	0	0	0
CYP2C9	S46963	9	8	8
CYP2C18	M61853	2	0	1
CYP2C19	M61854	**1800**	**2227**	**2199**
CYP2D6	M20403	**2901**	**2518**	**2284**
CYP3A4	M18907	**491**	11	15
CYP3A5	J04813	270	**2904**	1140
CYP3A7	D00408	8	5	**3467**

B

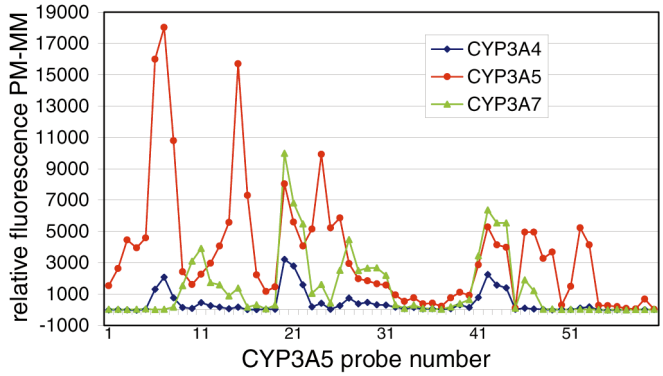

Fig. 2. Analysis of hybridization specificity utilizing the *CYP* gene family. Biotinylated in vitro transcripts from *CYP2A6*, *CYP2C19*, *CYP2D6*, and either *CYP3A4*, *CYP3A5*, or *CYP3A7* were hybridized at 30 pM each to the GeneChip "Merck-1." *A*: hybridization of each sample to 25-mer oligodeoxynucleotide probe pairs representing genes from the human CYP subfamilies: *CYP2A*, *CYP2C*, *CYP2D*, and *CYP3A*. Gene sequences are identified with GenBank accession numbers. Data from individual hybridizations are normalized to the levels of *CYP2A6*, *CYP2C19*, and *CYP2D6*. Homologous hybridization data are depicted in bold. Note significant heterologous hybridization to the *CYP3A5* gene. *B*: hybridization of *CYP3A4*, *CYP3A5*, and *CYP3A7* to 60 individual probe pairs representing *CYP3A5* on Affymetrix GeneChip "Merck-1." The *y*-axis represents the fluorescence differences for each probe pair (PM − MM).

for the *CYP3A5* gene compared with the long 3′-UT of the *CYP3A4* and *CYP3A7* genes. This short 3′-UT necessitated that the 1,000 bp region represented on the microarray occur primarily in the coding region of the gene. This region of the gene appears to permit heterologous hybridization despite showing lower sequence identities to *CYP3A4* and *CYP3A7* (88% and 89%, respectively) than the 92% identity shared by the 3′ ends of *CYP3A4* and *CYP3A7*.

Drug metabolism gene regulation. We further validated the application of DNA microarrays to drug safety by treating rats with four compounds that provoke well-characterized transcriptional responses among the *CYP* superfamily. 3MC, phenobarbital, dexamethasone, and clofibrate are classic inducers of the cytochrome *P*-450 subfamily members *CYP1A*, *CYP2B*, *CYP3A*, and *CYP4A*, respectively (7). Several members of the *CYP* gene families can be transcriptionally activated by xenobiotics through one of four receptor-dependent mechanisms. 3MC activates transcription of the *CYP1* family through the aromatic hydrocarbon (AH) receptor (35), phenobarbital activates transcription of the *CYP2B* and *CYP3A* family through the CAR (15), and dexamethasone activates transcription of the *CYP3A* family through the pregnane nuclear receptor (PXR; Ref. 4), and clofibrate activates transcription of the *CYP4A* subfamily through the peroxisome proliferator-activated receptor-α (PPARα; Ref. 29).

The results from the induction experiments in which male rats were treated with drug or vehicle are shown in Fig. 3. A regimen of intraperitoneal administration once daily for 3 days and harvest of livers at *day 4* was selected, based on prior experience, to represent the steady-state response to compounds. Hybridization samples from two animals per treatment were prepared and hybridized to the Merck Drug Safety Chip. Figure 3 includes all genes that were regulated by any of the compounds in these experiments. The results are presented as the mean expression profiles in livers from rats treated with 3MC, phenobarbital, dexamethasone, or clofibrate. Colors were assigned to data points to reflect twofold induction (red) or suppression (green) with a difference of ≥20 units in drug-treated samples relative to controls. Additional data points that fail one of these criteria, but that are consistent in replicate data and/or substantiated by the literature are colored light red or light green to avoid possible omissions. Several genes in Fig. 3 are homologous to other rat genes at >90% DNA:DNA identity, including *CYP2A1*:*CYP2A2*, *CYP2B1*:*CYP2B2*, *GSTA1*:*GSTA2*, and *HSST1*:*HSST2*. It is possible that data for these genes reflects heterologous hybridization, as suggested by the data in Fig. 2.

3MC is an aromatic hydrocarbon that induces the expression of *CYP1A1*, *CYP1A2*, and *CYP1B1* by activating the AH receptor. The AH receptor is a helix-loop-helix protein that belongs to the PAS (PER, Arnt, and SIM) family of transcription factors and regulates transcription of the CYP1 genes. The AH receptor becomes activated by binding to an aromatic hydrocarbon in the cytosol. The complex then translocates to the nucleus where it complexes with the nuclear factor Arnt. The activated ligand-receptor transcription factor complex then binds to the xenobiotic response element (XRE) in the *CYP1* gene promoter. Binding of the activated receptor-ligand complex activates transcription of the genes (16). *CYP1A1* is undetectable in the liver of control (vehicle-treated) rats (16) but was found to be highly expressed (induced) in the liver of 3MC-treated rats (Fig. 3). Induction of *CYP1A2* and *CYP1B1* were also observed in the livers from rats treated with 3MC. This is in agreement with published reports that clearly show that both *CYP1A2* and *CYP1B1* induction can occur by an AH receptor-dependent mechanism. In addition, several reports have indicated that both *CYP1A2* and *CYP1B1* induction can occur by an AH receptor-independent mechanism (26) possibly occurring through the AP1 transcription complex (22). *CYP2D4* was moderately induced by 3MC and by dexamethasone (Fig. 3). Regulation of *CYP2D4* has not been previously explored (14).

Induction of several phase II enzymes, *UGT1A6*, *GSTA1*, *GSTA2*, and *GSTM1*, was also observed in the liver recovered from rats treated with 3MC (Fig. 3). 3MC is known to induce expression of the UDP-glucuronosyl transferase gene *UGT1A6* (5) and glutathione-*S*-transferase gene *GSTA1* (25), by an AH receptor-dependent mechanism. The *GSTA2* and *GSTM1* genes are both regulated (induced) by the *CYP1A1* epoxide and hydroxylated metabolite(s) of 3MC. Both genes contain an antioxidant response element (ARE) in their promoter region. This *cis*-acting element has been shown to be responsive to the diol metabolites of 3MC that can redox cycle and produce a pro-oxidative environment (25). The glutathione-*S*-transferase genes *GSTA2* and *GSTM1* (19) were previously observed to be 3MC inducible in cultured rat hepatocytes.

The barbiturate phenobarbital is also a transcriptional inducer of the rat genes *CYP2B1*, *CYP2B2*, and *CYP3A1* (7). In mouse, phenobarbital induction of *Cyp2b10* requires the phenobarbital-response element (PBRE), an enhancer upstream of the *Cyp2b10* gene. CAR is a nuclear receptor that interacts with the RXR nuclear receptor to form CAR-RXR heterodimers which bind to the PBRE in response to phenobarbital treatment, suggesting CAR-RXR may play a role in phenobarbital induction of mouse *Cyp2b10* (15). The microarray data in Fig. 3 show the induction *CYP2B1*, *CYP2B2*, and *CYP3A1*. We observe a moderate but consistent suppression of *CYP2B3* by all four compounds. Little is known about *CYP2B3* function, but Yamada et al. (35) have reported expression and drug-mediated induction of *CYP2B3* in rat liver. *CYP2C7* is also reportedly induced by phenobarbital, but primarily in female rather than in male rats (7). No CAR-RXR response element has been identified in the *CYP3A1* promoter region.

Induction of several of the phase II enzymes was observed after treatment with phenobarbital. A significant increase in the specific mRNA for microsomal epoxide hydrolase (EHm), *UGT2B1*, *GSTA1*, *GSTA2*,

GSTA3, and *GSTM1*, was also observed in the liver recovered from rats treated with phenobarbital (Fig. 3). Phenobarbital is known to induce expression of the CYP2B genes by the fore-mentioned CAR-dependent mechanism. No PBRE sequence has been identified in the promoters for any of the phase II enzymes to date. In addition to the phase I and II enzyme induction, a significant increase in the cation transporter, *cMOAT*, was also observed. Little is known about its regulation in rat liver.

Dexamethasone is a synthetic glucocorticoid mimetic that is known to induce expression of several *CYP3A* subfamily genes. Recent reports have described the identification and cloning of a nuclear receptor (PXR, the pregnane nuclear receptor) that can bind a variety of chemical structures leading to the induction of *CYP3A1* in the liver. This nuclear receptor has been identified in mouse (mPXR), in rat (rPXR), in rabbit (rbPXR) and in humans (PAR, or SXR) (17) (4). In a manner similar to that of the CAR, the PXR can also form heterodimeric complexes with the RXR and bind to a *cis*-acting sequence in the promoter region of the target gene. PXR-responsive *cis*-acting regulatory elements have been identified in the promoters of *CYP3A* genes in each of these species. In agreement with these findings, we observed a marked induction of *CYP3A1* and *CYP3A18* genes in the liver from rats treated with dexamethasone (Fig. 3). A moderate induction of *CYP2B1* and *CYP2B2* is also evident, as reported by Ronis et al. (24).

Induction of several of the phase II enzymes was also observed after treatment with dexamethasone. Significant increases in the specific mRNAs for *UGT1A6*, *UGT2B1*, *GSTA1*, *GSTA2*, *GSTM1* and for sulfotransferases *PST*, *HSST1*, and *HSST2* were detected in the mRNA recovered from the livers of rats treated with dexamethasone (Fig. 3). Dexamethasone is known to induce expression of the *CYP3A* genes by the aforementioned PXR-dependent mechanism. No *cis*-acting sequence has been identified in the promoters of any of

Gene	Acc. #	Control	Clofib	Dex	Phenob	3MC
Phase I						
CYP1A1	X00469	1	1	2	2	93
CYP1B1	U09540	1	1	0	1	32
CYP1A2	K02422	110	40	51	43	530
CYP2A1	J02669	27	64	15	15	10
CYP2A2	J04187	140	190	43	59	74
CYP2B1	M37134	2	47	14	270	0
CYP2B2	K00996	7	40	33	130	16
CYP2B3	M20406	74	35	28	25	25
CYP2D4	AB008425	4	2	11	7	15
CYP3A1	M10161	11	24	76	60	8
CYP3A18	X79991	15	17	47	12	10
*CYP4A1**	M14972	18	156	11	11	22
CYP4A2	M57719	8	100	6	6	6
CYP4A3	M33936	43	150	29	21	27
CYP4F1	M94548	55	29	38	66	46
CYP4F4	U39206	11	8	18	21	13
CYP4F6	U39208	17	6	6	21	5
EHc	X65083	5	29	2	0	1
EHm	M26125	57	36	59	220	87
Phase II						
UGT1A6	J02612	25	57	58	41	72
UGT2B1	M13506	4	3	30	47	2
GlPx1	M21210	130	100	50	150	100
GSTA1	K01931	150	66	250	270	270
GSTA2	M25891	14	7	35	44	38
GSTA3	S72505	30	39	27	57	34
GSTM1	M11719	47	7	140	200	140
GSTM2	J02592	54	22	79	76	59
EST	M86758	56	86	27	48	44
PST	X52883	170	250	290	101	90
HSST1	M31363	23	15	45	9	27
HSST2	M33329	8	7	60	6	7
Phase III						
NTCP	M77479	42	37	25	31	37
CMOAT	D86086	17	3	14	34	11
HSLIP	X51415	14	29	12	6	8
FACO	J02752	36	430	22	17	22
BE	K03249	2	410	0	4	1
CPT2	U88295	12	41	13	9	10
MCACD	J02791	39	80	26	28	27
KCAT	J02749	42	680	19	60	60
LCAT	U62803	46	22	72	41	26
APOA1	M00001	240	140	560	340	260
APOA4	X13629	46	0	190	84	22
APOC1	X15512	600	320	440	740	300
PEPCK	K03248	32	9	50	23	4
DALS	J04044	1	27	1	5	6
PRCR	D28966	7	44	0	4	0
HSP70	L16764	14	64	22	21	15
SODxc	X68041	10	30	13	16	13

Fig. 3. Gene regulation profiles of 3-methylcholanthrene (3MC), phenobarbital, dexamethasone, and clofibrate in male rat livers. Expression data are shown in units of relative fluorescence for those genes that respond to one or more drugs within gene families that encode drug metabolism enzymes. Upregulation events are red, and downregulation events are green. Events which do not meet explicit criteria (differ by ≥20 units, and by a ratio of ≥2-fold) but are consistent in replicate data sets are light red or light green. Numbers represent mean expression level measurements in two separate microarrays and are given in arbitrary units. GenBank accession numbers representing each gene are given under the column heading "Acc. #." Gene abbreviations are as follows: *CYP*, cytochrome *P*-450; *EHc*, cytosolic epoxide hydrolase; *EHm*, mitochondrial epoxide hydrolase; *UGT*, UDP-glucuronosyltransferase, *GlPx*, glutathione peroxidase; *GST*, glutathione sulfotransferase; *EST*, estradiol sulfotransferase; *PST*, phenol/aryl sulfotransferase; *HSST*, hydroxysteroid sulfotransferase; *NTCP*, Na-taurocholate cotransporting polypeptide; *CMOAT*, canalicular multispecific organic anion transporter; *FACO*, fatty acid/acyl CoA oxidase; *BE*, peroxisomal enoyl-CoA hydratase/3-hydroxyacyl CoA dehydrogenase "bifunctional enzyme"; *HSLIP*, hormone-sensitive lipase; *FACO*, acyl-CoA oxidase; *BE*, bifunctional enzyme; *CPT2*, carnitine palmitoyl transferase II; *MCACD*, medium chain acyl-CoA dehydrogenase; *KCAT*, 3-ketoacyl-CoA thiolase; *LCAT*, lecithin:cholesterol acyltransferase; *APO*, apolipoproteins; *PEPCK*, phospho*enol*pyruvate carboxykinase C; *DALS*, delta-aminolevulinate synthase; *PRCR*, prostacyclin or prostaglandin I_2 receptor; *HSP70*, heat shock protein 70; *SODxc*, extracellular superoxide dismutase. *Eight of 20 probe pairs for *CYP4A1* were masked due to gene-nonspecific hybridization. This appears to result from a 185-bp perfect identity between the 3′ ends of the *CYP4A1* and *Apolipoprotein B* gene sequences (GenBank accession nos. M14972 and M27440, respectively; unpublished comparison).

the phase II enzymes to date. In addition to the phase I and phase II enzyme induction, a significant decrease in the levels of mRNA for sulfotransferase *EST* and phase III transporter *NTCP* were also observed. Little is known about their regulation in rat liver.

Clofibrate is a lipid-lowering agent that triggers peroxisome proliferation in rodents. The increase in enzyme expression that accompanies the proliferation of peroxisomes is mediated through a fourth nuclear receptor, PPARα. The peroxisome proliferator compounds are considered agonists of PPARα. As described previously for the CAR and PXR receptors, the PPARα also forms heterodimeric complexes with RXR. The complex can bind agonist and interact with the *cis*-acting sequence [peroxisome proliferator response element (PPRE)] in the promoter of responsive genes. PPARα is also activated by cellular long-chain fatty acid derivatives, stimulating β-oxidation of long-chain fatty acids in peroxisomes. Clofibrate and other PPARα agonists are known to induce members of the *CYP4A* subfamily. Figure 3 shows transcriptional induction by clofibrate of *CYP4A1*, *CYP4A2*, and *CYP4A3*. Additionally, a small but significant increase in the expression of *CYP2B1*, *CYP2B2*, and *CYP3A1* was observed.

Induction of several of the phase II enzymes was also observed after treatment with clofibrate. Significant increases in the specific mRNA for *UGT1A6* and sulfotransferase *PST* were also observed in the liver of rats treated with clofibrate (Fig. 3). Clofibrate is known to induce expression of the *CYP4A* genes by the aforementioned PPAR-dependent mechanism. No *cis*-acting PPRE sequence has been identified in the promoters of any of the phase II enzymes to date. We also observed a significant decrease in the mRNA for several of the phase II and III enzymes. Significant decreases were seen for *GSTA1*, *GSTM1*, *GSTM2*, and the transporter *cMOAT*. Little is known about their regulation in rat liver. Each of the four compounds examined directly regulates several drug metabolism genes, through binding to a nuclear receptor or the AH receptor, thus activating the promoters of the genes. Figure 3 shows that each compound also regulates a series of other drug metabolism genes by unknown mechanisms. Many of these are likely to be indirect mechanisms, including competition of the agonized-nuclear receptor for other transcription factors, such as RXR, CBP/p300, and histone acetylases. Such indirect mechanisms may also include primary regulation of a gene product that alters metabolism of the natural ligands for nuclear receptors, altering expression of secondary genes.

Metabolic energy and stress-related gene regulation. In addition to drug-metabolizing genes, Fig. 3 indicates induction or suppression of genes that indicate toxicological events and genes that regulate sugar and lipid metabolism. 3MC and clofibrate treatments, for example, downregulate lecithin:cholesterol acyltransferase (*LCAT*), apolipoprotein CI (*APOC1*), apolipoprotein AIV (*APOA4*), and phospho*enol*pyruvate carboxykinase C (*PEPCK*). These regulatory events indicate decreased lipid turnover, as well as decreased gluconeogenesis mediated by PEPCK, in the liver. Consistent with this data for 3MC, AH receptor agonists have been found to cause lipid accumulation within hepatocytes in vivo (3) and to regulate lipid metabolism via the AH receptor in cultured fibroblasts (1), although the mechanism remains unclear. Induction of apolipoprotein genes *APOA1* and *APOA4* by phenobarbital and dexamethasone was also observed (Fig. 3), consistent with increased high-density lipoprotein levels and increased apolipoprotein AI expression in response to these agents in previous reports (9, 23).

Clofibrate is known to globally increase lipoprotein uptake and increase fatty acid β-oxidation in both peroxisomes and mitochondria in liver (31). The increased lipoprotein uptake is reflected in Fig. 3 by induction of hormone-sensitive lipase (*HSLIP*). Similarly, decreased lipid levels in serum are suggested by downregulation of apolipoprotein genes *APOA1*, *APOA4*, and *APOC1*. Clofibrate suppression of *APOA1* expression is opposite to that in humans, but is consistent with previous studies in male rodents (32). Increased lipid β-oxidation in response to clofibrate is indicated by induction of peroxisomal genes acyl-CoA oxidase (*FACO*), bifunctional enzyme (*BE*), and 3-ketoacyl-CoA thiolase (*KCAT*); and mitochondrial genes carnitine palmitoyl transferase II (*CPT2*) and medium chain acyl-CoA dehydrogenase (*MCACD*).

Induction of mitochondrial delta-aminolevulinate synthase (*DALS*) indicates increased heme synthesis. Such heme likely supports increased CYP4A enzymes, mitochondrial electron transport proteins, or both. Fatty acid β-oxidation by peroxisomes and mitochondria is thought to cause oxidative stress by producing reactive oxygen intermediates. Evidence of oxidative stress includes induction of the extracellular Cu-Zn superoxide dismutase (*SODxc*), and heat shock protein 70 (*HSP70*), as observed in hepatic oxidative stress caused by CCl_4 (28). Induction of the SODxc gene by peroxisome proliferators has not been previously reported, although Yoo et al. (36) report induction of the rat intracellular Cu-Zn superoxide dismutase (*SOD1*) gene by arachidonic acid.

Figure 3 indicates clofibrate induction of the prostacyclin or prostaglandin I_2 receptor (*PRCR*). Prostaglandin I_2 mediates blood vessel dilation and inhibits platelet activation (21). Induction of the *PRCR* may thus be a marker for the antithrombotic activity of clofibrate (21). Induction of the *PRCR* appears to be part of a larger shift in the balance of prostaglandin species in clofibrate-treated liver. *CYP4A1*, *CYP4A2*, and *CYP4A3* genes are induced by clofibrate (Fig. 3) and show varying degrees of ω-hydroxylase activity on prostaglandins (2) as well as fatty acids. The latter fatty acid ω-hydroxylase activity commits fatty acids to peroxisomal degradation. The CYP4F enzymes also can form or degrade various prostaglandins (6, 16), although their activities are not well characterized. Figure 3 shows a trend toward downregulation of the *CYP4F1*, *CYP4F4*, and *CYP4F6* genes by clofibrate. Thus, although the physiological implications are not clear, it appears likely that regulation of the *CYP4A*, *CYP4F*, and *PRCR* genes by clofibrate may decrease

thrombotic activity by altering the prostaglandin balance in rats.

Quantitation of mRNA levels by Q-RT-PCR. An independent method, TaqMan Q-RT-PCR (33), was used to check changes in mRNA levels for selected genes. Since mRNA levels were determined in each sample relative to an internal control, 18S rRNA, the Q-RT-PCR data is expressed as a ratio of mRNA in treated relative to control samples. This method employs a pair of gene sequence-specific PCR primers to amplify cDNA derived from (rat liver) total RNA. During each PCR cycle, the PCR product is quantitated using a third oligonucleotide "probe." This probe anneals to the PCR product between the two primers and is degraded by the template-dependent exonuclease activity of *Taq* polymerase. The amount of PCR product is quantitated by the exonucleolytic release of a fluorescent dye linked to the probe. Based on microarray data from Fig. 3, the following genes were selected to check the observed magnitudes of large changes and the reliability of moderate changes: *CYP1A1*, *CYP3A18*, *CYP4A1*, *GSTM1*, *BE*, and *APOA1*. A comparison of quantitation by microarray and by Q-RT-PCR is presented in Fig. 4.

Both microarray and Q-RT-PCR indicate a marked induction of *CYP1A1* mRNA by 3MC: >9.3-fold by microarray and ~5,000-fold by Q-RT-PCR. Q-RT-PCR data also indicate comparatively moderate induction of *CYP1A1* by dexamethasone and phenobarbital, at 23-fold and 7.4-fold, respectively. In contrast, the corresponding microarray data for dexamethasone and phenobarbital effects on *CYP1A1* fall below the threshold of detection. Since the *CYP1A1* transcript occurs at much lower levels in the control samples than the other five genes in this study (data not shown), these data illustrate the sensitivity of the PCR. Both techniques indicate induction of *CYP3A18* by dexamethasone, 3.1-fold by microarray and 6.2-fold by Q-RT-PCR. Similarly, both techniques indicate induction of *CYP4A1* by clofibrate, at 8.7-fold by microarray and 47-fold by Q-RT-PCR. The difference in quantitation between these latter two samples may arise from the low and therefore imprecise control levels measured by the microarray assay or from imprecision in the Q-RT-PCR assay.

Gene	Control	Clofib	Dex	Phenob	3MC	Assay
CYP1A1	BDT	BDT	BDT	BDT	≥9.3-fold	gene chip
	1-fold	1.6-fold	23-fold**	7.4-fold*	5300-fold**	Q-RT-PCR
CYP3A18	1-fold	1.1-fold	3.1-fold	0.80-fold	0.67-fold	gene chip
	1-fold	0.60-fold	6.2-fold*	0.68-fold	0.88-fold	Q-RT-PCR
CYP4A1	1-fold	8.7-fold	0.61-fold	0.61-fold	1.2-fold	gene chip
	1-fold	47-fold*	0.85-fold	0.44-fold	0.86-fold	Q-RT-PCR
GSTM1	1-fold	0.21-fold	3.0-fold	4.3-fold	3.0-fold	gene chip
	1-fold	0.41-fold	3.8-fold*	7.3-fold*	2.9-fold*	Q-RT-PCR
BE	BDT	≥41-fold	BDT	BDT	BDT	gene chip
	1-fold	78-fold*	0.35-fold*	1.6-fold	1.2-fold	Q-RT-PCR
ApoA1	1-fold	0.58-fold	2.3-fold	1.4-fold	1.1-fold	gene chip
	1-fold	0.94-fold	3.8-fold*	1.5-fold	1.7-fold	Q-RT-PCR

Fig. 4. Comparison of gene expression data by microarray and quantitative RT-PCR (Q-RT-PCR). Microarray data derived from Fig. 3 are shown as treated/control ratios in the *top* row beside each gene name. Microarray data points below 10 were converted to a minimum threshold value of 10 relative fluorescence units to calculate ratios. Data points below 10 fluorescence units are marked BDT for "below detection threshold." Q-RT-PCR data are shown in the *bottom* row beside each gene name as a ratio relative to the control samples. Gene names and drugs are as in Fig. 3. *Significantly different from control at 0.05 level by ANOVA test. **Significantly different from control at 0.001 level by ANOVA test.

For *GSTM1*, both techniques indicate moderate suppression by clofibrate and moderate induction by the other three compounds. Both techniques also indicate sharp induction of *BE* by clofibrate, at ≥41-fold by microarray and 78-fold by Q-RT-PCR. Although control levels of *BE* were not reliably measured by microarray, Q-RT-PCR indicates a moderate suppression of *BE* mRNA by dexamethasone. For *APOA1*, both techniques indicate induction by dexamethasone and phenobarbital, but Q-RT-PCR data were too imprecise to confirm or deny the 0.58-fold suppression of *APOA1* by clofibrate indicated by microarray.

Validation of the microarray results for these six genes by Q-RT-PCR showed qualitative agreement overall, yet illustrated fundamental differences between the two techniques. The microarray data failed to register expression of *CYP1A1* and *BE* without strong induction by 3MC, whereas Q-RT-PCR reproducibly detects all five genes in all samples (Fig. 4). The sensitivity of the microarray technology allows detection of gene transcripts down to ~1 part in 300,000 (18). This "detection threshold" can account for the lower ratios of induction indicated by microarray data for 3MC induction of *CYP1A1* and for clofibrate induction of *BE*. This threshold may also account for moderate differences in apparent induction ratios of *CYP3A18* by dexamethasone, *CYP4A1* by clofibrate, and *GSTM1* by phenobarbital. Alternatively, some of these differences may have resulted from imprecision in the Q-RT-PCR. Microarray technology has the principle advantage over Q-RT-PCR of examining expression of hundreds or thousands of genes in each experiment (18). Thus the microarray can be used to search many genes for those that respond to a stimulus, and Q-RT-PCR can be used in a complementary way, to confirm and extend observations on a few selected genes.

Conclusions. We have evaluated the microarray technology for use in determining how the rat liver responds to drug treatments at the mRNA level. The technology allowed discrimination of individual genes within cytochrome *P*-450 gene subfamilies up to ~90% DNA identities. This discrimination was accomplished by rational selection of oligonucleotide probes that were gene specific. Three genes from the *CYP3A* subfamily showing ~90% DNA identities were not fully distinguished. A subset of the 25-mer probe pairs from *CYP3A5* were identified that show *CYP3A5* gene-specific hybridization relative to *CYP3A4* and *CYP3A7*. This combination of rational sequence selection and empirical hybridization analysis enabled us to unambiguously identify a subset of oligonucleotide probes

that are gene specific for the most problematic gene, *CYP3A5*.

Responses of rat genes relevant to drug metabolism and drug safety were measured using microarray technology and four much studied xenobiotic compounds. These gene expression events concur with numerous previous observations recorded in the literature and concur qualitatively with Q-RT-PCR assays from the same study, thus validating application of microarray technology to drug metabolism and drug safety. Several novel gene regulation responses were also recorded, including induction of markers that elucidate toxicological responses such as *HSP70* and *SODxc*.

Advances in DNA microarray technologies and mammalian genome sequencing will soon allow quantitative assessment of expression profiles of all genes in the selected tissues. The ability to predict phenotypic outcomes from gene expression profiles is currently in its infancy, however, and will require additional bioinformatic tools. Such tools will facilitate information gathering from literature and gene databases as well as integration of expression data with animal physiology studies.

We thank Donghui Zhang, Ting-Chuan Wang, and Daniel Holder for statistics support and Robert L. Phillips for critical review of the manuscript.

REFERENCES

1. **Alexander DL, Ganem LG, Fernandez-Salguero P, Gonzalez F, and Jefcoate CR.** Aryl-hydrocarbon receptor is an inhibitory regulator of lipid synthesis and of commitment to adipogenesis. *J Cell Sci* 111: 3311–3322, 1998.
2. **Aoyama T, Hardwick JP, Imaoka S, Funae Y, Gelboin HV, and Gonzalez FJ.** Clofibrate-inducible rat hepatic P450s IVA1 and IVA3 catalyze the omega- and (omega-1)-hydroxylation of fatty acids and the omega-hydroxylation of prostaglandins E1 and F2 alpha. *J Lipid Res* 31: 1477–1482, 1990.
3. **Barak Y, Nelson MC, Ong ES, Jones YZ, Ruiz-Lozano P, Chien KR, Koder A, and Evans RM.** PPAR gamma is required for placental, cardiac, and adipose tissue development. *Mol Cell* 4: 585–595, 1999.
4. **Bertilsson G, Heidrich J, Svensson K, Asman M, Jendeberg L, Sydow-Backman M, Ohlsson R, Postlind H, Blomquist P, and Berkenstam A.** Identification of a human nuclear receptor defines a new signaling pathway for CYP3A induction. *Proc Natl Acad Sci USA* 95: 12208–12213, 1998.
5. **Bock KW, Gschaidmeier H, Heel H, Lehmkoster T, Munzel PA, Raschko F, and Bock-Hennig B.** AH receptor-controlled transcriptional regulation and function of rat and human UDP-glucuronosyltransferase isoforms. *Adv Enzyme Regul* 38: 207–222, 1998..
6. **Bylund J, Finnstrom N, and Oliw EH.** Gene expression of a novel cytochrome P450 of the CYP4F subfamily in human seminal vesicles. *Biochem Biophys Res Commun* 261: 169–174, 1999.
7. **Correia MA.** Rat and human liver cytochromes P450. In: *Cytochrome P450s, Structure, Mechanism, and Biochemistry* (2nd ed.), edited by Ortiz de Montellano PR. New York: Plenum, 1995, p. 610–611.
8. **Der SD, Zhou A, Williams BR, and Silverman RH.** Identification of genes differentially regulated by interferon alpha, beta, or gamma using oligonucleotide arrays. *Proc Natl Acad Sci USA* 95: 15623–15628, 1998.
9. **Elshourbagy NA, Boguski MS, Liao WS, Jefferson LS, Gordon JI, and Taylor JM.** Expression of rat apolipoprotein A-IV and A-I genes: mRNA induction during development and in response to glucocorticoids and insulin. *Proc Natl Acad Sci USA* 82: 8242–8246, 1985.
10. **Fodor SP, Rava RP, Huang XC, Pease AC, Holmes CP, and Adams CL.** Multiplexed biochemical assays with biological chips. *Nature* 364: 555–556, 1993.
11. **Gerhold D, Rushmore T, and Caskey CT.** DNA chips: promising toys have become powerful tools. *Trends Biochem Sci* 24: 168–173, 1999.
12. **Gonzalez FJ.** Overview of experimental approaches for study of drug metabolism and drug-drug interactions. *Adv Pharmacol* 43: 255–277, 1997.
13. **Haining RL, Hunter AP, Veronese ME, Trager WF, and Rettie AE.** Allelic variants of human cytochrome P450 2C9: baculovirus-mediated expression, purification, structural characterization, substrate stereoselectivity, and prochiral selectivity of the wild-type and I359L mutant forms. *Arch Biochem Biophys* 333: 447–458, 1996.
14. **Hiroi T, Imaoka S, Chow T, and Funae Y.** Tissue distributions of CYP2D1, 2D2, 2D3 and 2D4 mRNA in rats detected by RT-PCR. *Biochim Biophys Acta* 1380: 305–312, 1998.
15. **Honkakoski P, Zelko I, Sueyoshi T, and Negishi M.** The nuclear orphan receptor CAR-retinoid X receptor heterodimer activates the phenobarbital-responsive enhancer module of the CYP2B gene. *Mol Cell Biol* 18: 5652–5658, 1998.
16. **Jin R, Koop DR, Raucy JL, and Lasker JM.** Role of human CYP4F2 in hepatic catabolism of the proinflammatory agent leukotriene B4. *Arch Biochem Biophys* 359: 89–98, 1998.
17. **Kliewer SA, Moore JT, Wade L, Staudinger JL, Watson MA, Jones SA, McKee DD, Oliver BB, Willson TM, Zetterstrom RH, Perlmann T, and Lehmann JM.** An orphan nuclear receptor activated by pregnanes defines a novel steroid signaling pathway. *Cell* 92: 73–82, 1998.
18. **Lockhart DJ, Dong H, Byrne MC, Follettie MT, Gallo MV, Chee MS, Mittmann M, Wang C, Kobayashi M, Horton H, and Brown EL.** Expression monitoring by hybridization to high-density oligonucleotide arrays. *Nat Biotechnol* 14: 1675–1680, 1996.
19. **Maheo K, Antras-Ferry J, Morel F, Langouet S, and Guillouzo A.** Modulation of glutathione S-transferase subunits A2, M1, and P1 expression by interleukin-1β in rat hepatocytes in primary culture. *J Biol Chem* 272: 16125–16132, 1997.
20. **Marton MJ, DeRisi JL, Bennett HA, Iyer VR, Meyer MR, Roberts CJ, Stoughton R, Burchard J, Slade D, Dai H, Bassett DE Jr., Hartwell LH, Brown PO, and Friend SH.** Drug target validation and identification of secondary drug target effects using DNA microarrays. *Nat Med* 4: 1293–1301, 1998.
21. **Metz G, Sim AK, McCraw AP, and Cleland ME.** Effect of etofylline clofibrate on experimental thrombus formation and prostacyclin activation. *Arzneimittelforschung* 36: 1363–1365, 1986.
22. **Quattrochi LC, Shih H, and Pickwell GV.** Induction of the human CYP1A2 enhancer by phorbol ester. *Arch Biochem Biophys* 350: 41–48, 1998.
23. **Reddy MN.** Effect of anticonvulsant drugs on plasma total cholesterol, high-density lipoprotein cholesterol, and apolipoproteins A and B in children with epilepsy. *Proc Soc Exp Biol Med* 180: 359–363, 1985.
24. **Ronis MJ, Rowlands JC, Hakkak R, and Badger TM.** Altered expression and glucocorticoid-inducibility of hepatic CYP3A and CYP2B enzymes in male rats fed diets containing soy protein isolate. *J Nutr* 129: 1958–1965, 1999.
25. **Rushmore TH, King RG, Paulson KE, and Pickett CB.** Regulation of glutathione S-transferase Ya subunit gene expression: identification of a unique xenobiotic-responsive element controlling inducible expression by planar aromatic compounds. *Proc Natl Acad Sci USA* 87: 3826–3830, 1990.
26. **Sakuma T, Ohtake M, Katsurayama Y, Jarukamjorn K, and Nemoto N.** Induction of CYP1A2 by phenobarbital in the livers of aryl hydrocarbon-responsive and -nonresponsive mice. *Drug Metab Dispos* 27: 379–384, 1999.
27. **Schena M.** Genome analysis with gene expression microarrays. *Bioessays* 18: 427–431, 1996.
28. **Schiaffonati L and Tiberio L.** Gene expression in liver after toxic injury: analysis of heat shock response and oxidative stress-inducible genes. *Liver* 17: 183–191, 1997.

29. **Simpson AE.** The cytochrome P450 4 (CYP4) family. *Gen Pharmacol* 28: 351–359, 1997.
30. **Soares MB, Bonaldo MF, Jelene P, Su L, Lawton L, and Efstratiadis A.** Construction and characterization of a normalized cDNA library. *Proc Natl Acad Sci USA* 91: 9228–9232, 1994.
31. **Staels B, Dallongeville J, Auwerx J, Schoonjans K, Leitersdorf E, and Fruchart JC.** Mechanism of action of fibrates on lipid and lipoprotein metabolism. *Circulation* 98: 2088–2093, 1998.
32. **Vu-Dac N, Chopin-Delannoy S, Gervois P, Bonnelye E, Martin G, Fruchart JC, Laudet V, and Staels B.** The nuclear receptors peroxisome proliferator-activated receptor α and Rev-erbα mediate the species-specific regulation of apolipoprotein A-I expression by fibrates. *J Biol Chem* 273: 25713–25720, 1998.
33. **Wang T and Brown MJ.** mRNA quantification by real time TaqMan polymerase chain reaction: validation and comparison with RNase protection. *Anal Biochem* 269: 198–201, 1999.
34. **Whitlock JP and Denison MS.** Induction of cytochrome P450 enzymes that metabolize xenobiotics. In: *Cytochrome P450s, Structure, Mechanism, and Biochemistry* (2nd ed.), edited by Ortiz de Montellano PR. New York: Plenum, 1995, p. 367.
35. **Yamada H, Minematsu Y, Nakamura T, Mise M, Fujisaki H, and Oguri K.** Brucine as a potent inducer of CYP2B3, the third member of the CYP2B subfamily P450 in rats. *Biol Pharm Bull* 19: 291–293, 1996.
36. **Yoo HY, Chang MS, and Rho HM.** Induction of the rat Cu/Zn superoxide dismutase gene through the peroxisome proliferator-responsive element by arachidonic acid. *Gene* 234: 87–91, 1999.